GEO-DEEP 9300: Introduction to receiver functions

Valerie Maupin

Many figures from IRIS training school lecture from Anne Sheehan (2006)
and from Stein and Wysession:

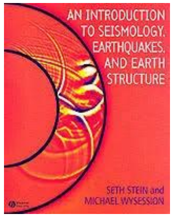

Receiver functions: «RFs»

Goal : detect interfaces in the subsurface

Reflection seismics:

Figure 1.1-5: Demonstration of the seismic reflection method.

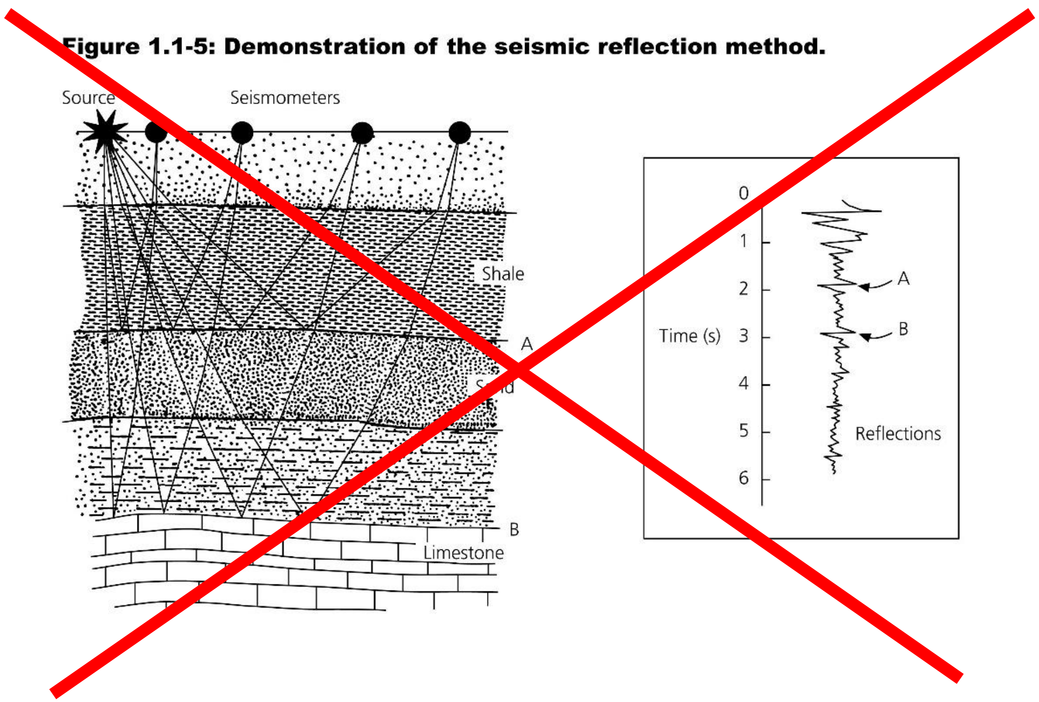

Figure 1.1-3: Example of seismogram, showing accompanying ray paths.

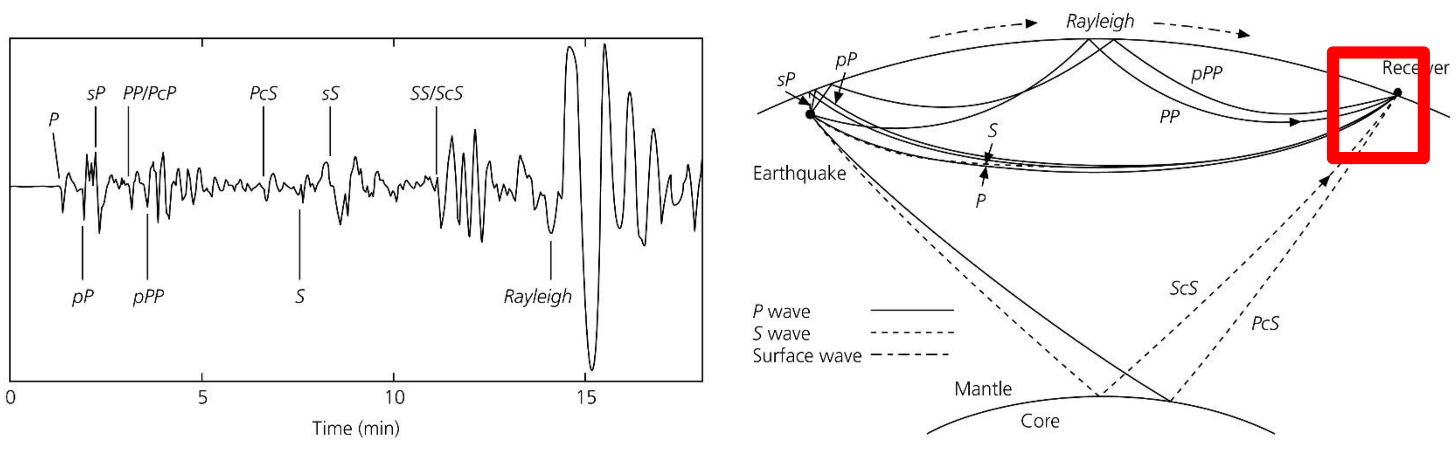

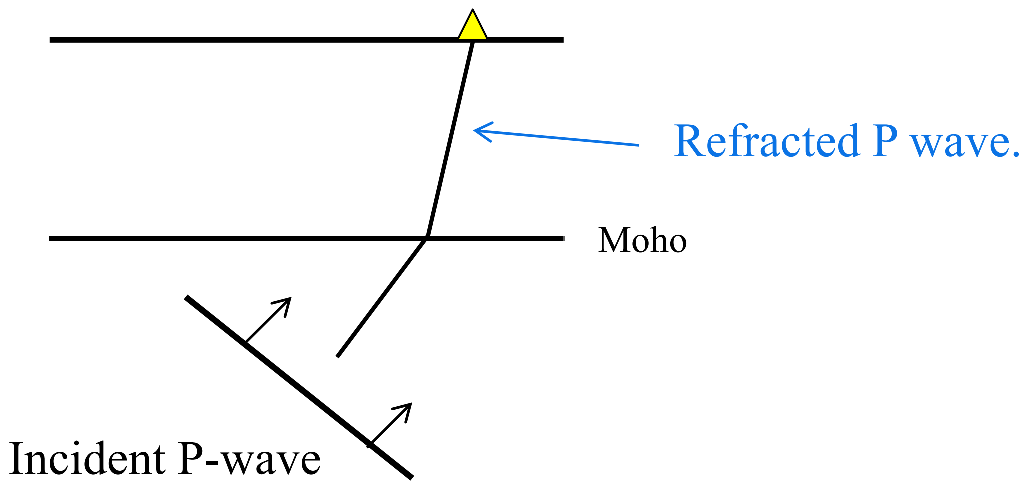
Refracted P wave.
Moho
Incident P-wave

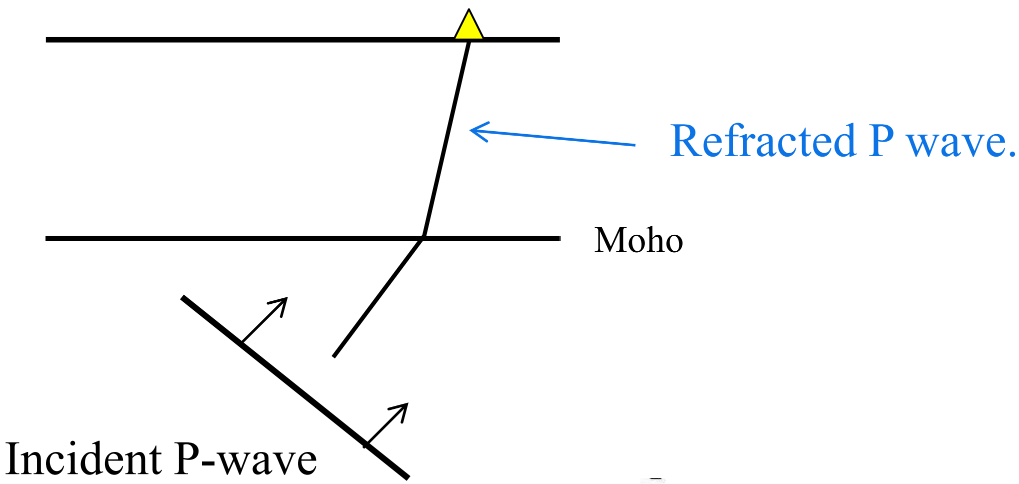
Refracted P wave.
Moho
Incident P-wave

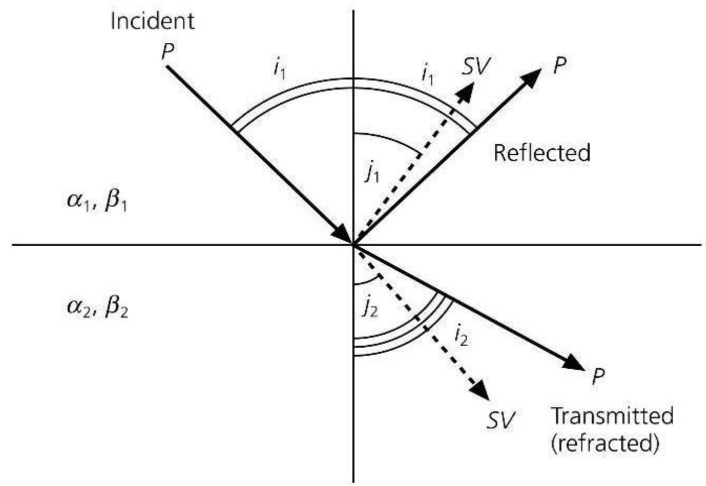
Incident
P
i_1
i_1
SV
P
Reflected
j_1
α_1, β_1
α_2, β_2
j_2
i_2
P
SV
Transmitted
(refracted)

Figure 6.3-7: Diagram of the receiver function approach.

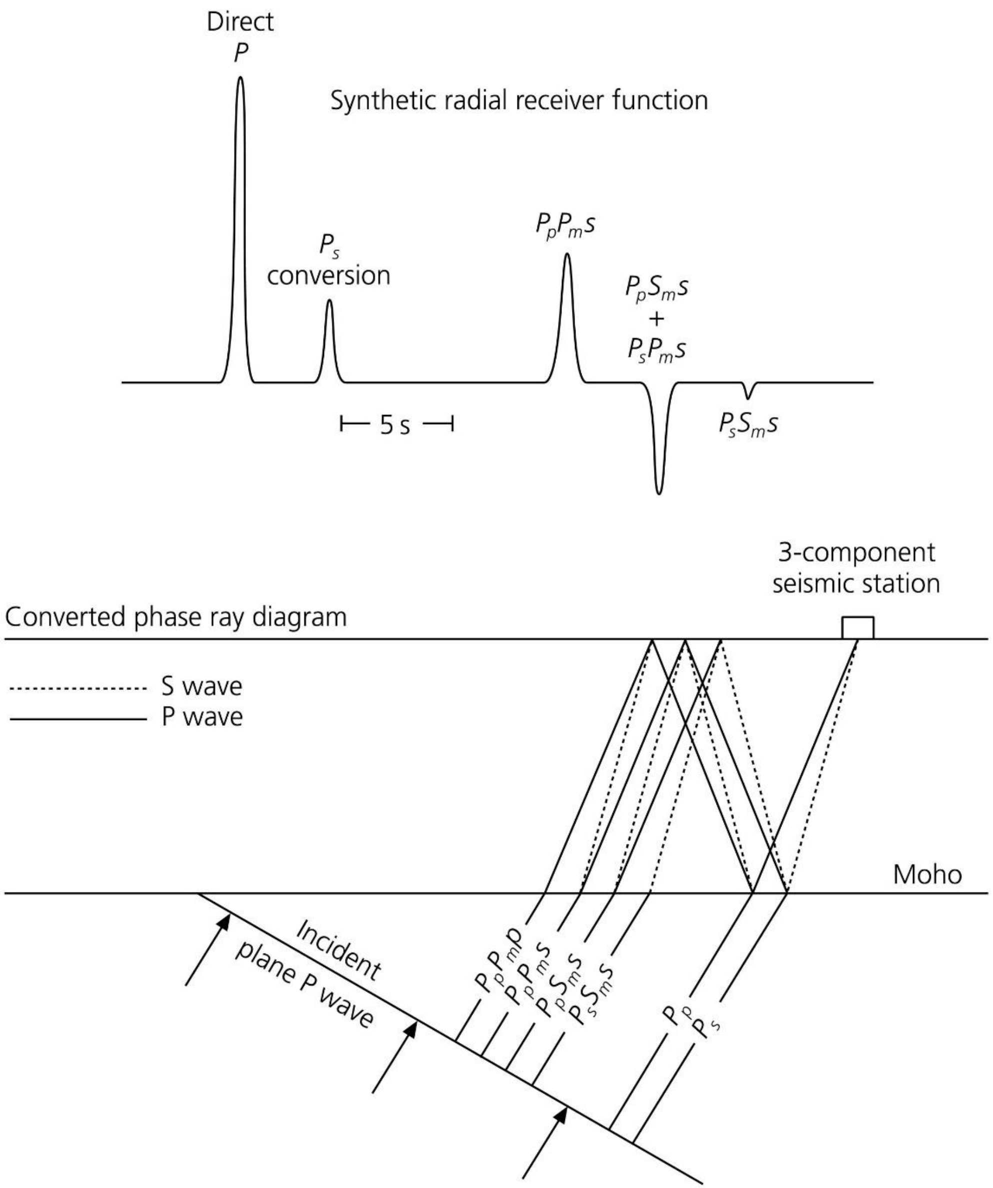

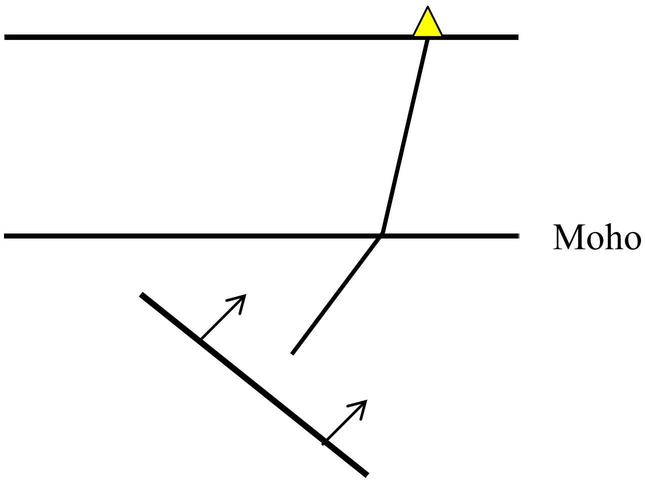

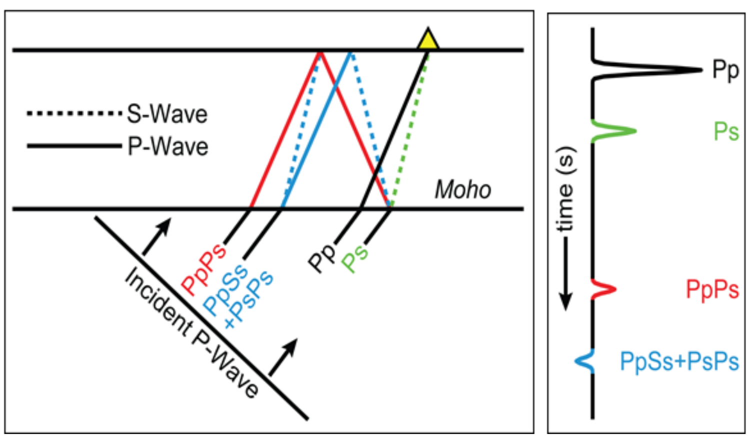

Reverberations may interfere with first arrival

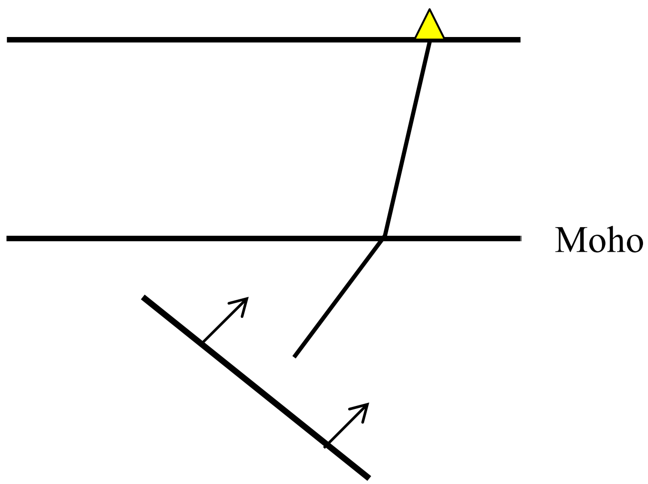

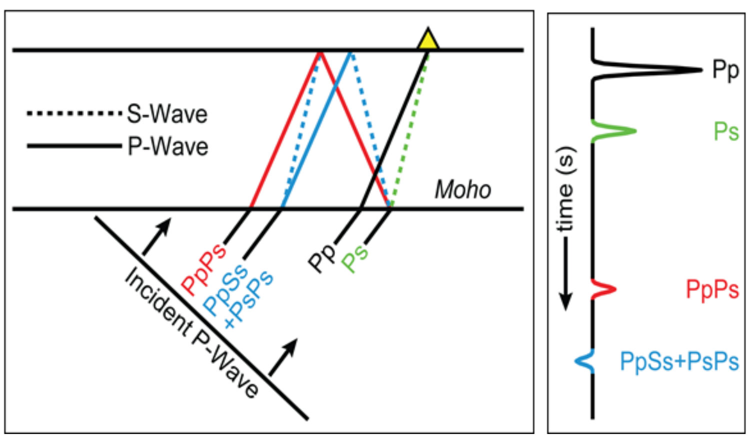

Sediments may bring additional phases

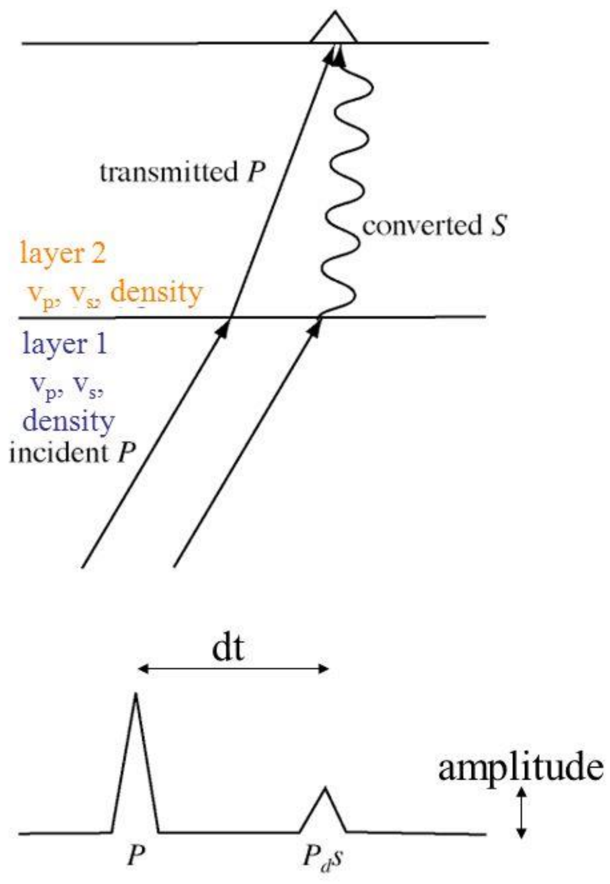

converted pulse:

delay time dt depends on depth of interface and v_p, v_s of top layer

amplitude depends on velocity contrast (mostly) and density contrast (weakly) at the interface

converted arrival:
"+" bump = bottom slow, top fast
"-" bump = bottom fast, top slow

receiver functions are sensitive to discontinuity structure

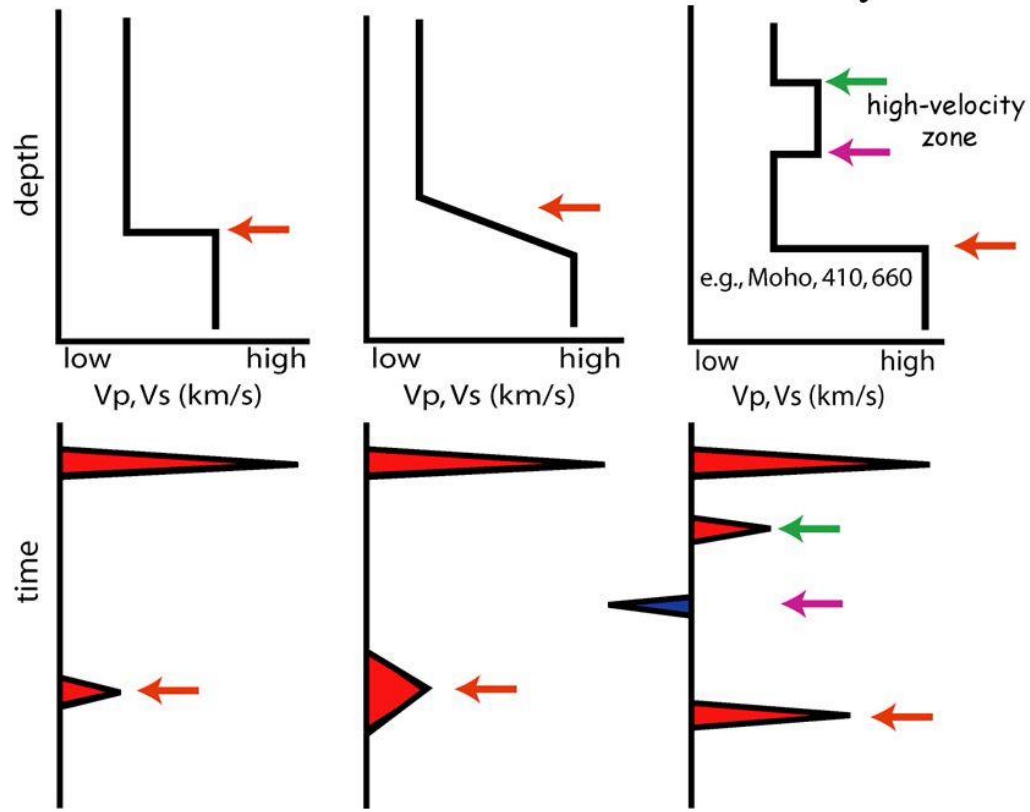

A single receiver function - hard to interpret

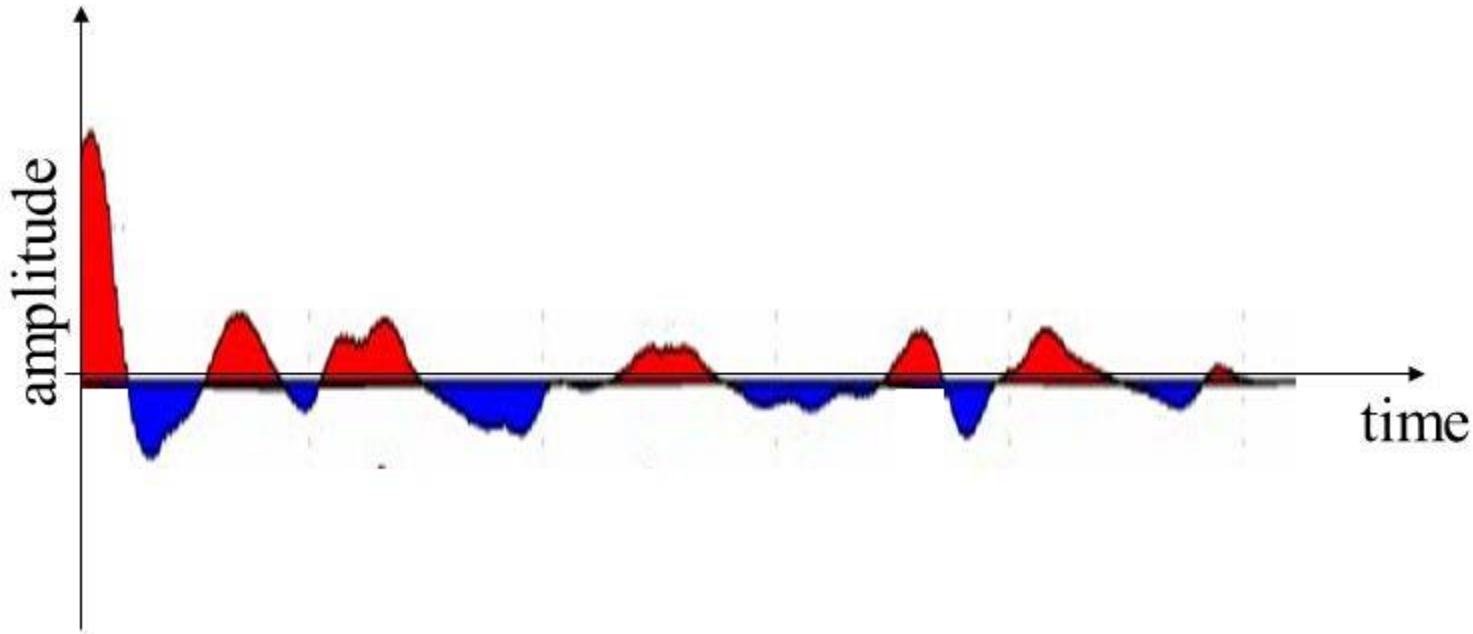

one receiver function per earthquake
-function of slowness (incidence angle)
-function of backazimuth (unless flat layered isotropic case)

UNIVERSITY OF OSLO

unfortunately, incident P is not a nice simple bump:

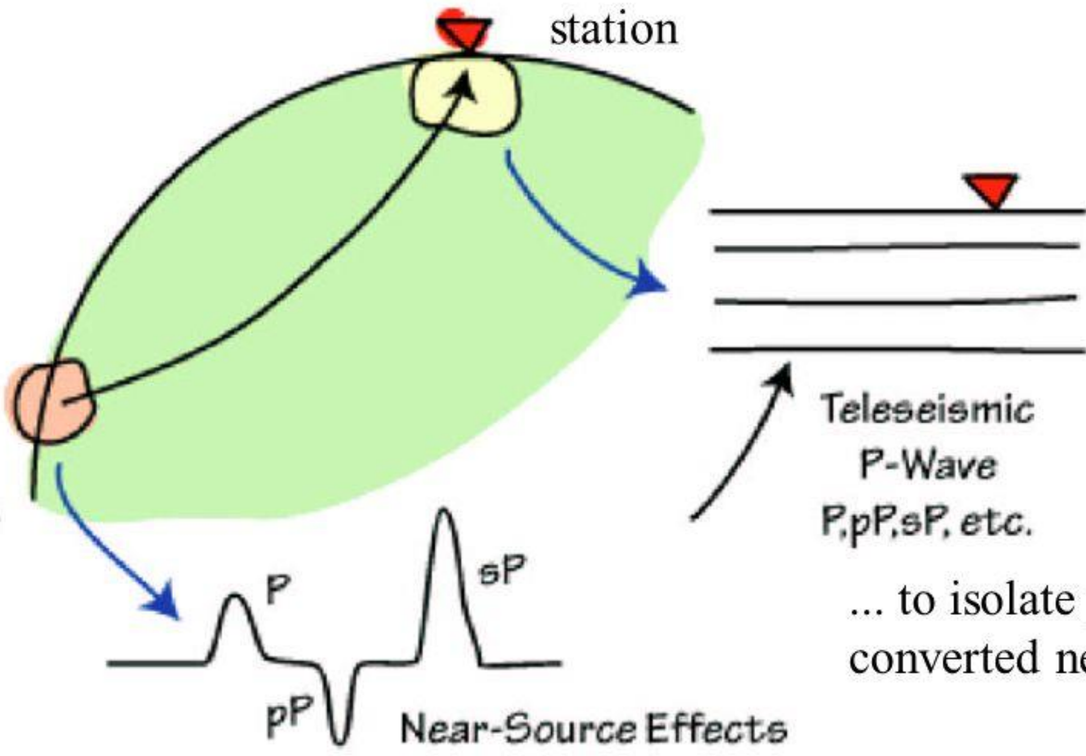

... to isolate phases converted near station

need to remove these bits ...

UNIVERSITY OF OSLO

Deconvolution of the source function

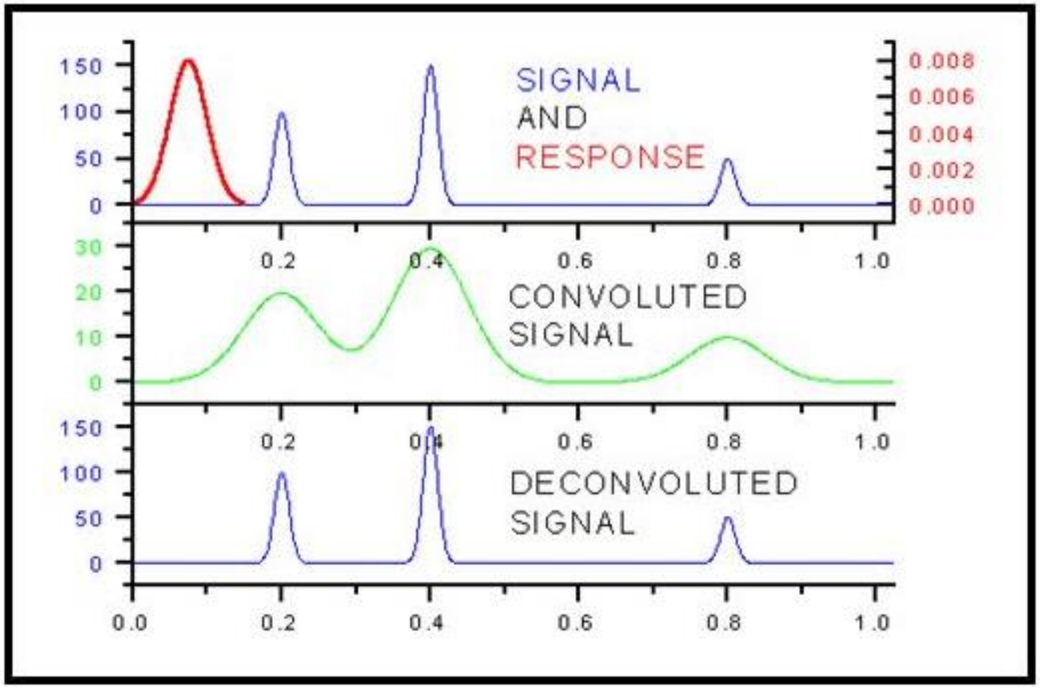

UNIVERSITY OF OSLO

Stack of events: average over azimuth

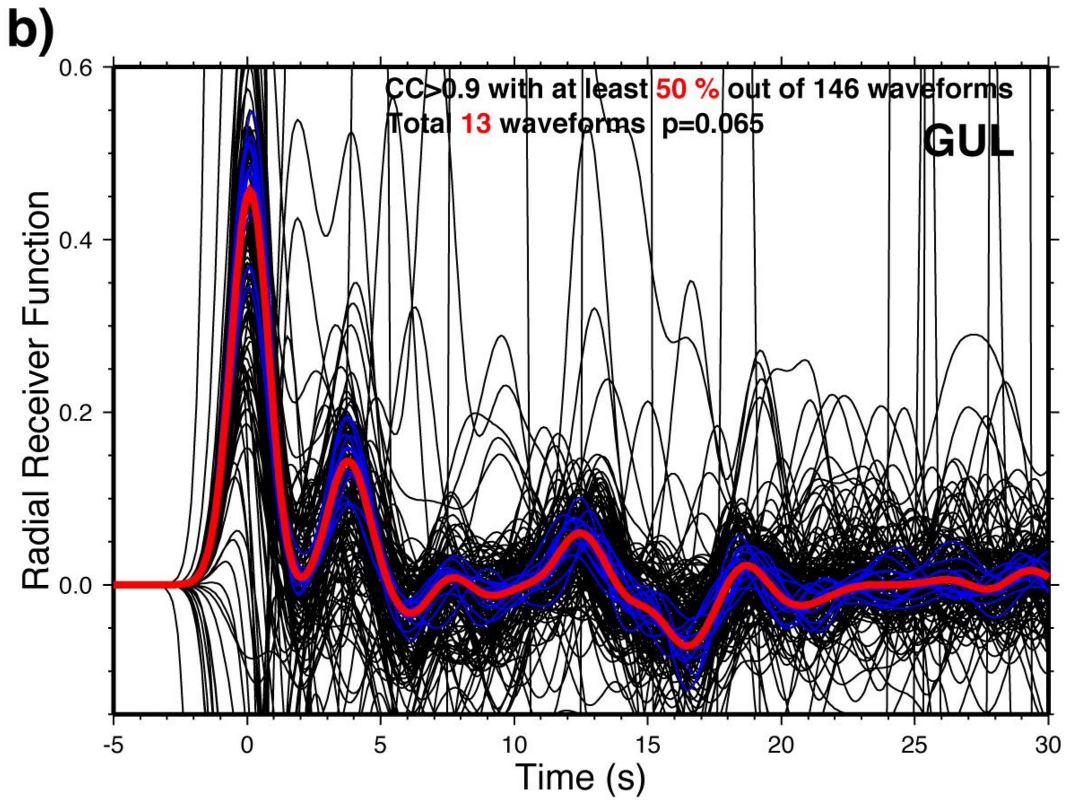

from Tkalcic et al., 2010

Can RF show a sharp lithosphere-asthenosphere boundary?

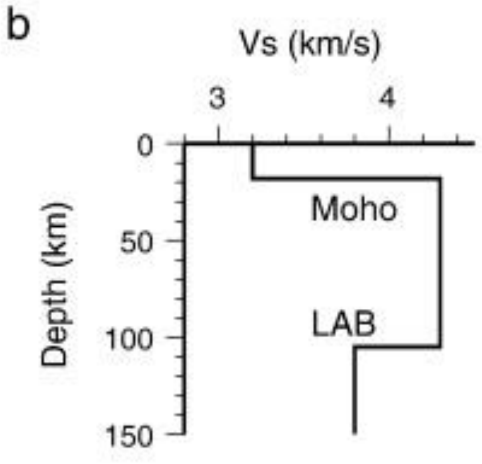

Kind et al.., 2012

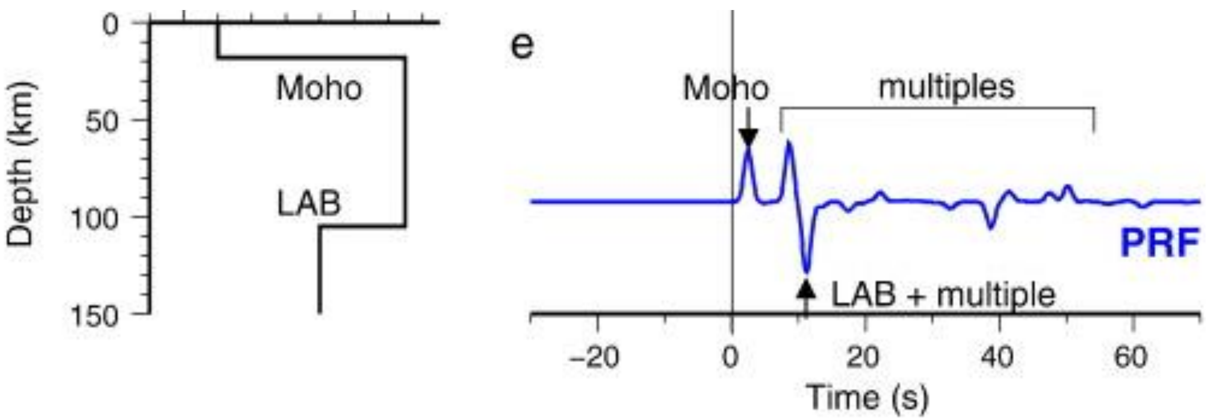

Kind et al.., 2012

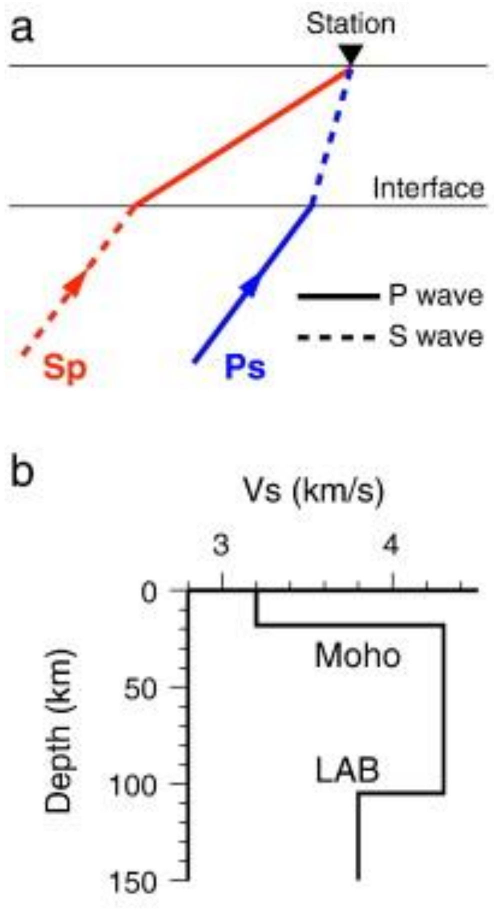

Kind et al.., 2012

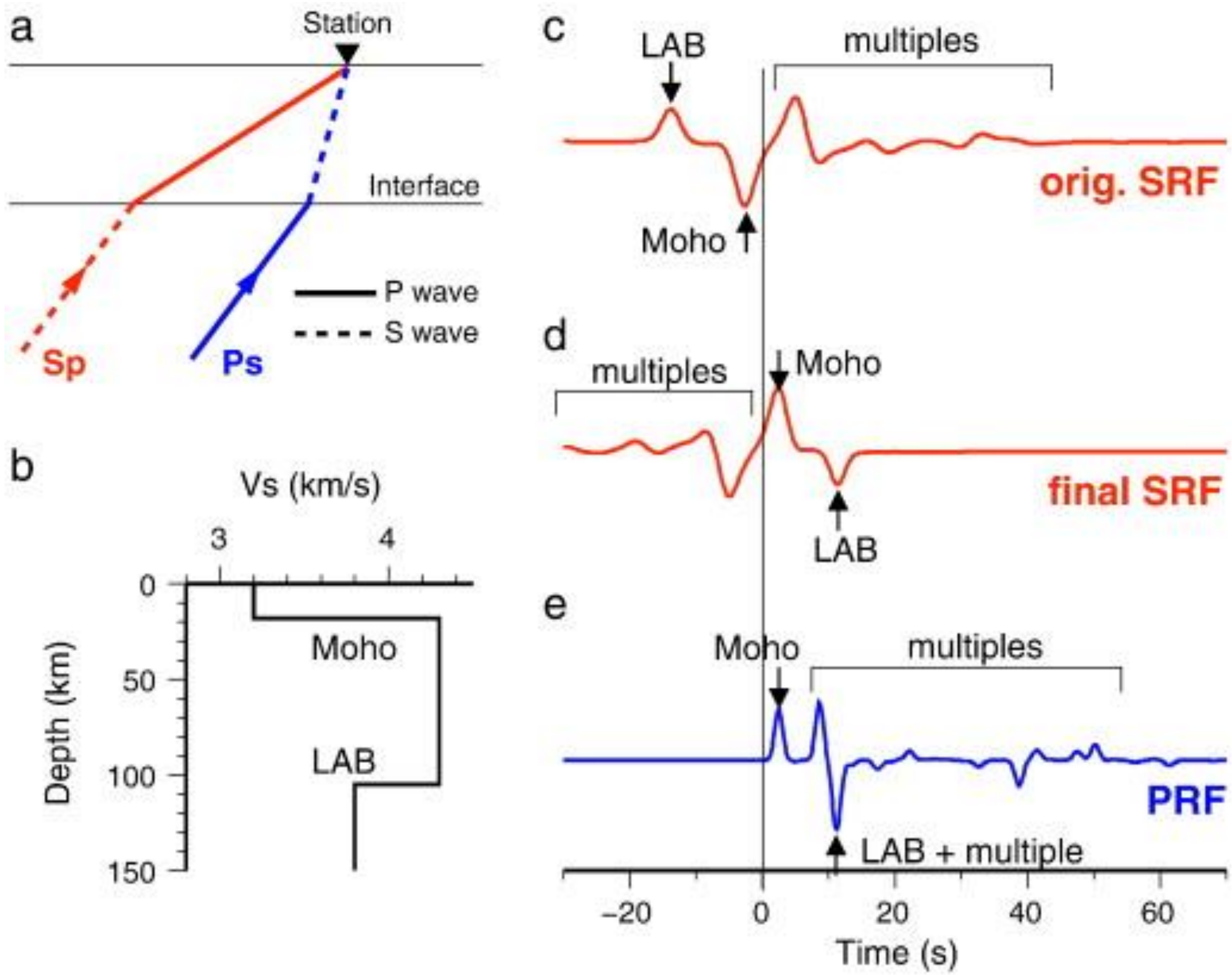

Kind et al.., 2012

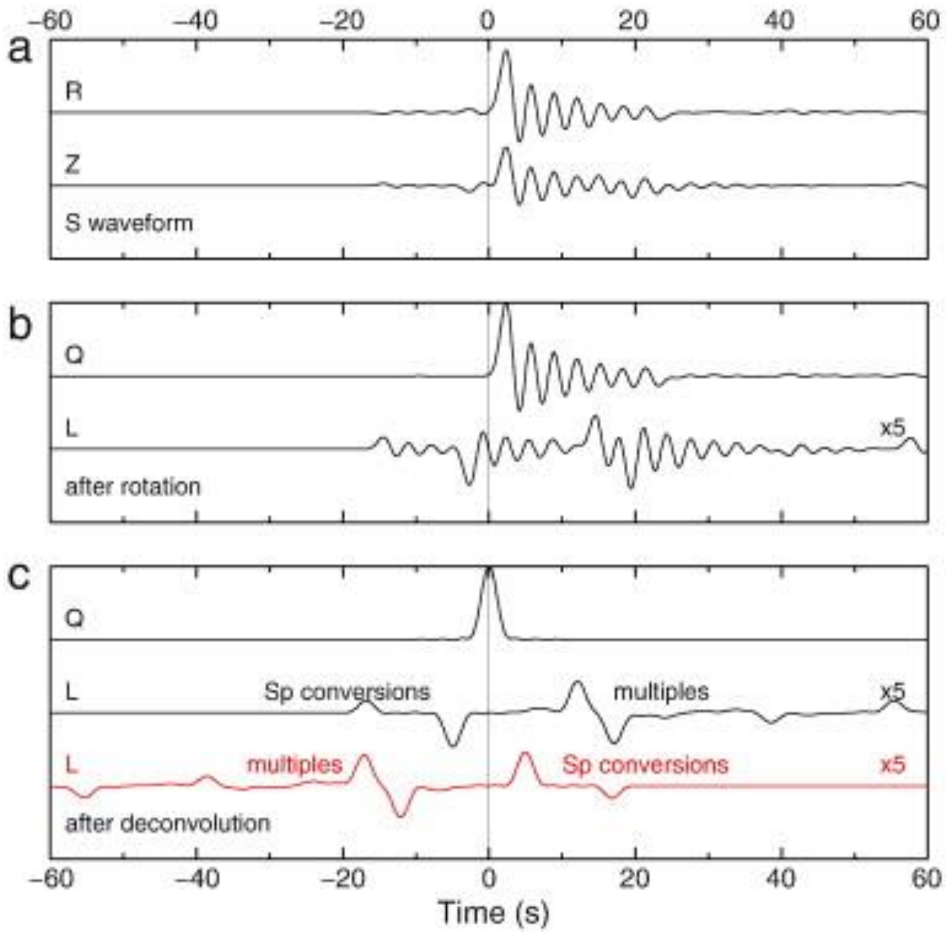

Kind et al.., 2012

UNIVERSITY OF OSLO

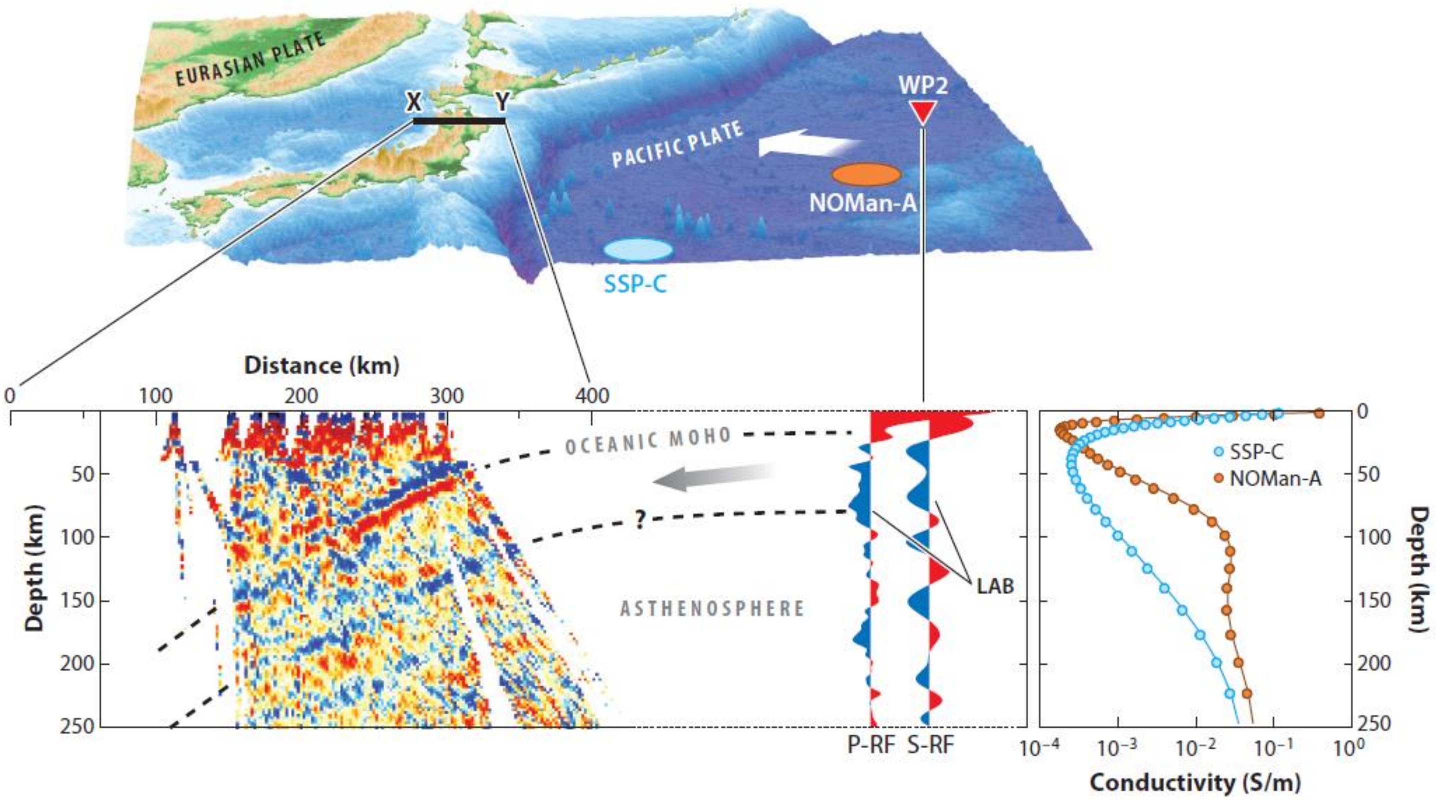

Figure 11

Lithosphere–asthenosphere system at a subduction zone: Shown are a P-RF image using dense land seismic data of Hi-net from Japan and a P-RF and S-RF image for the seafloor borehole station WP2, adapted from Kawakatsu et al. (2009). Also shown are the regional electrical conductivity profiles in two areas, NOMan-A and SSP-C; these data are from Baba et al. (2013). Abbreviations: LAB, lithosphere–asthenosphere boundary; NOMan, Normal Oceanic Mantle Project; P-RF, P-receiver function; S-RF, S-receiver function; SSP, Stagnant Slab Project.

Kawakatsu and Utada., 2017

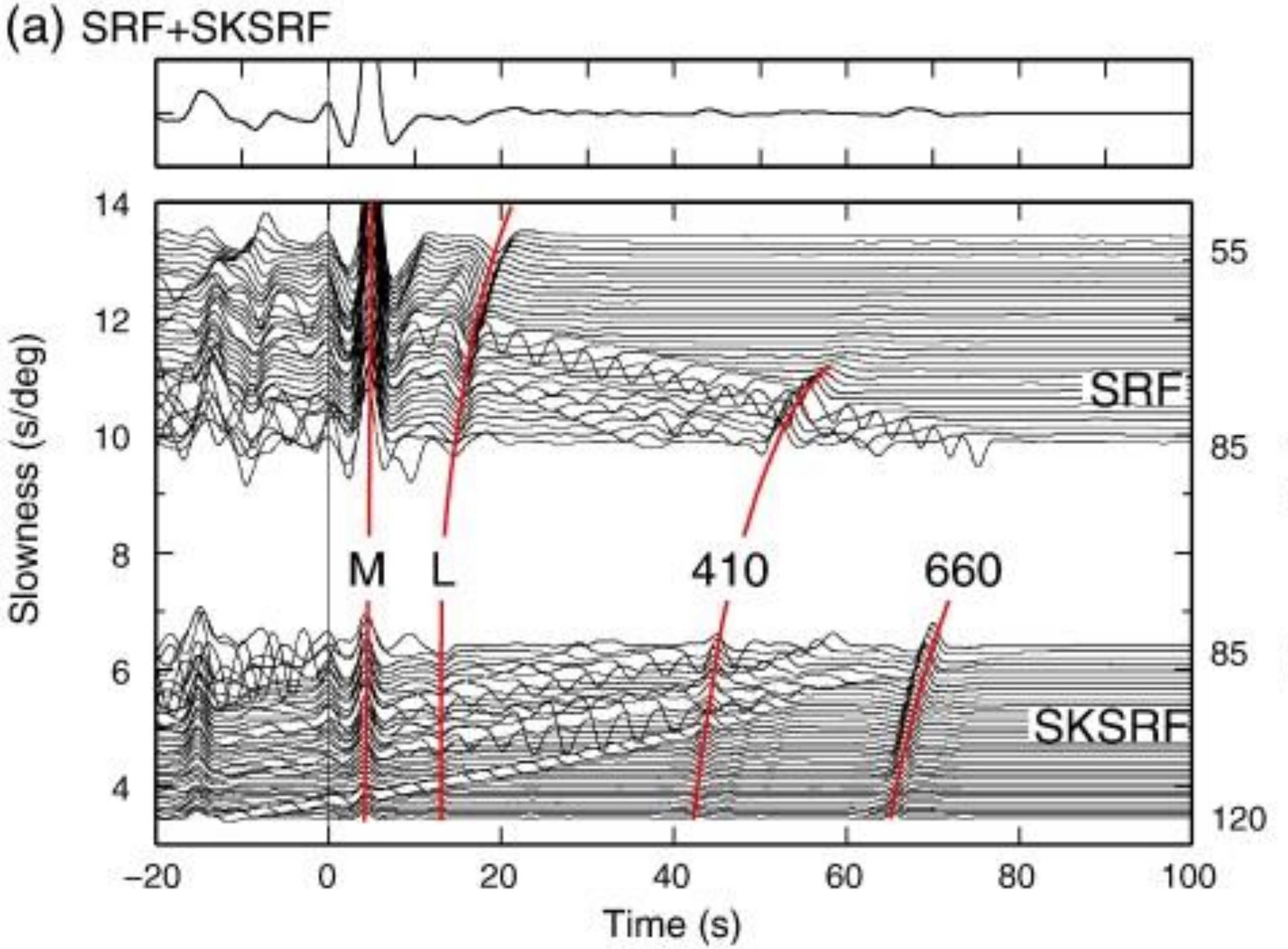

Kind et al.., 2012

UNIVERSITY OF OSLO

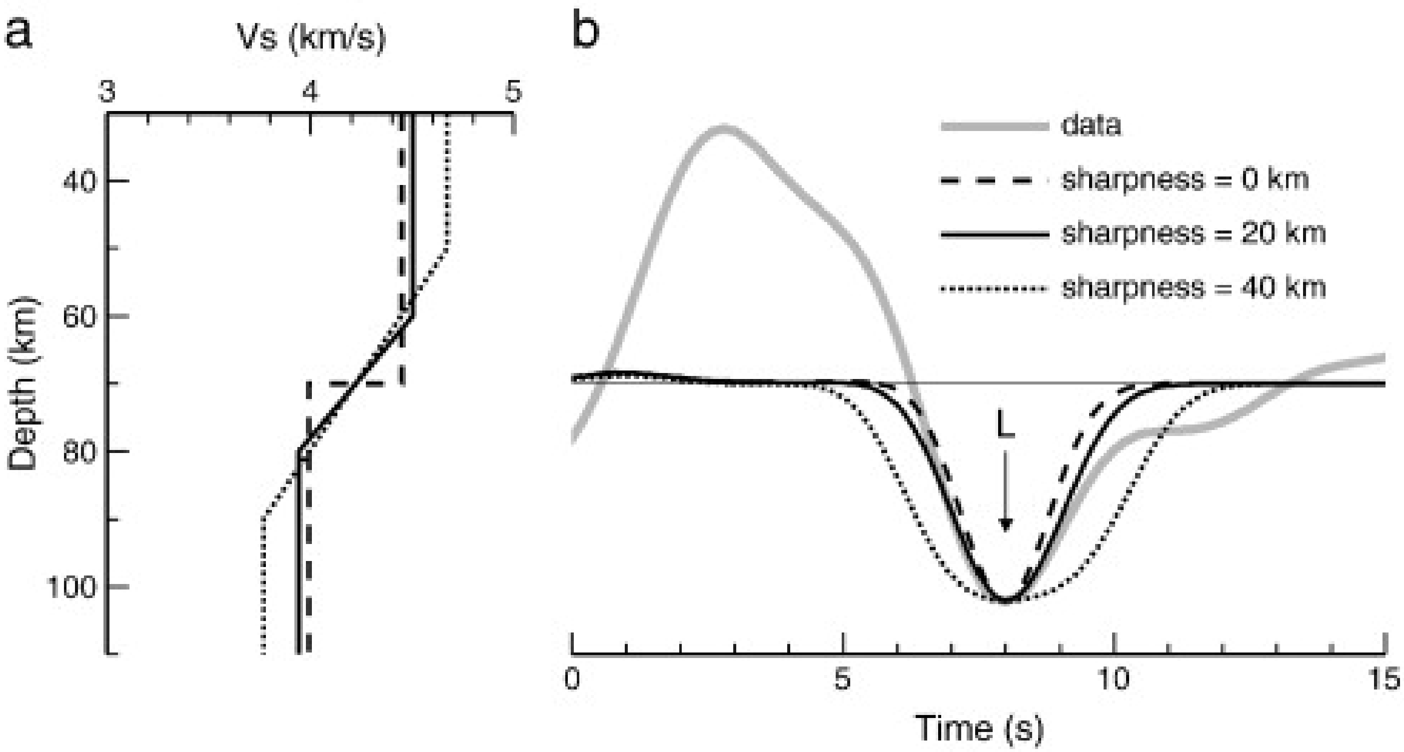

Kind et al.., 2012

Gradient of the LAB

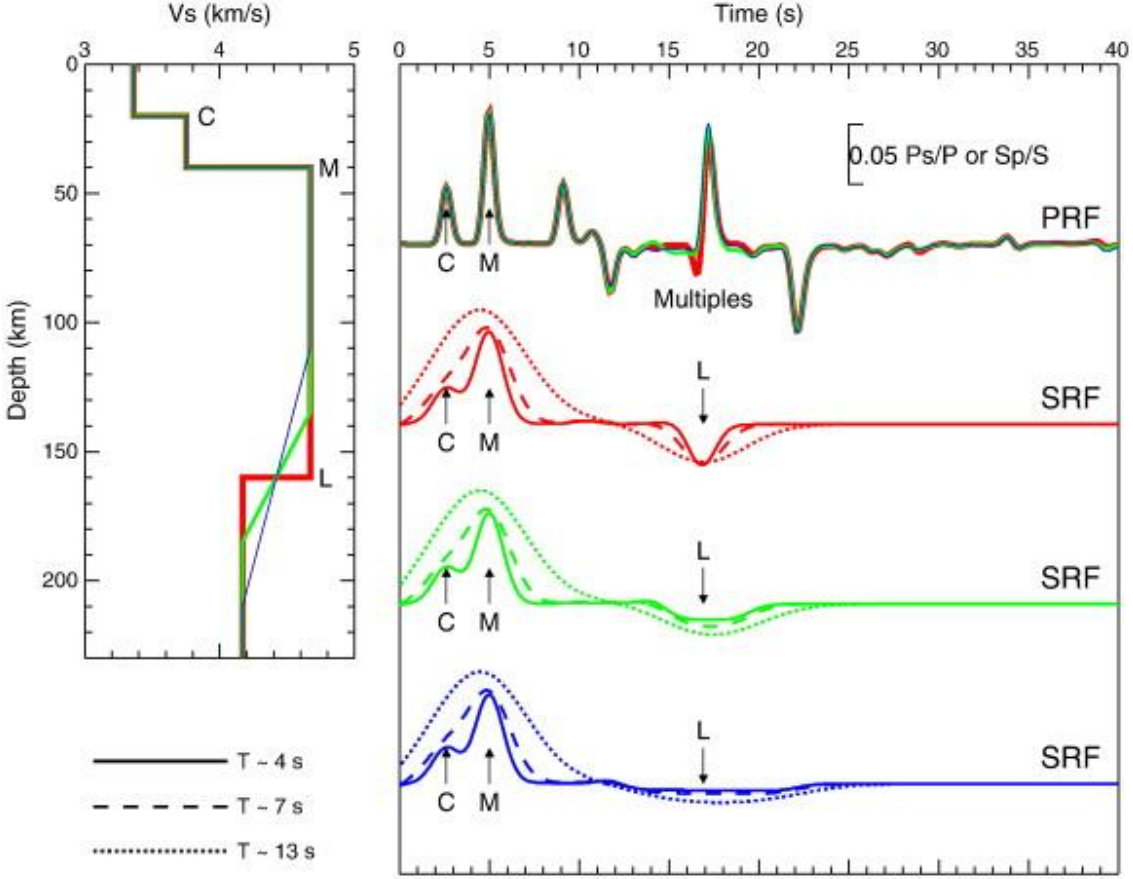

Kind et al.., 2012

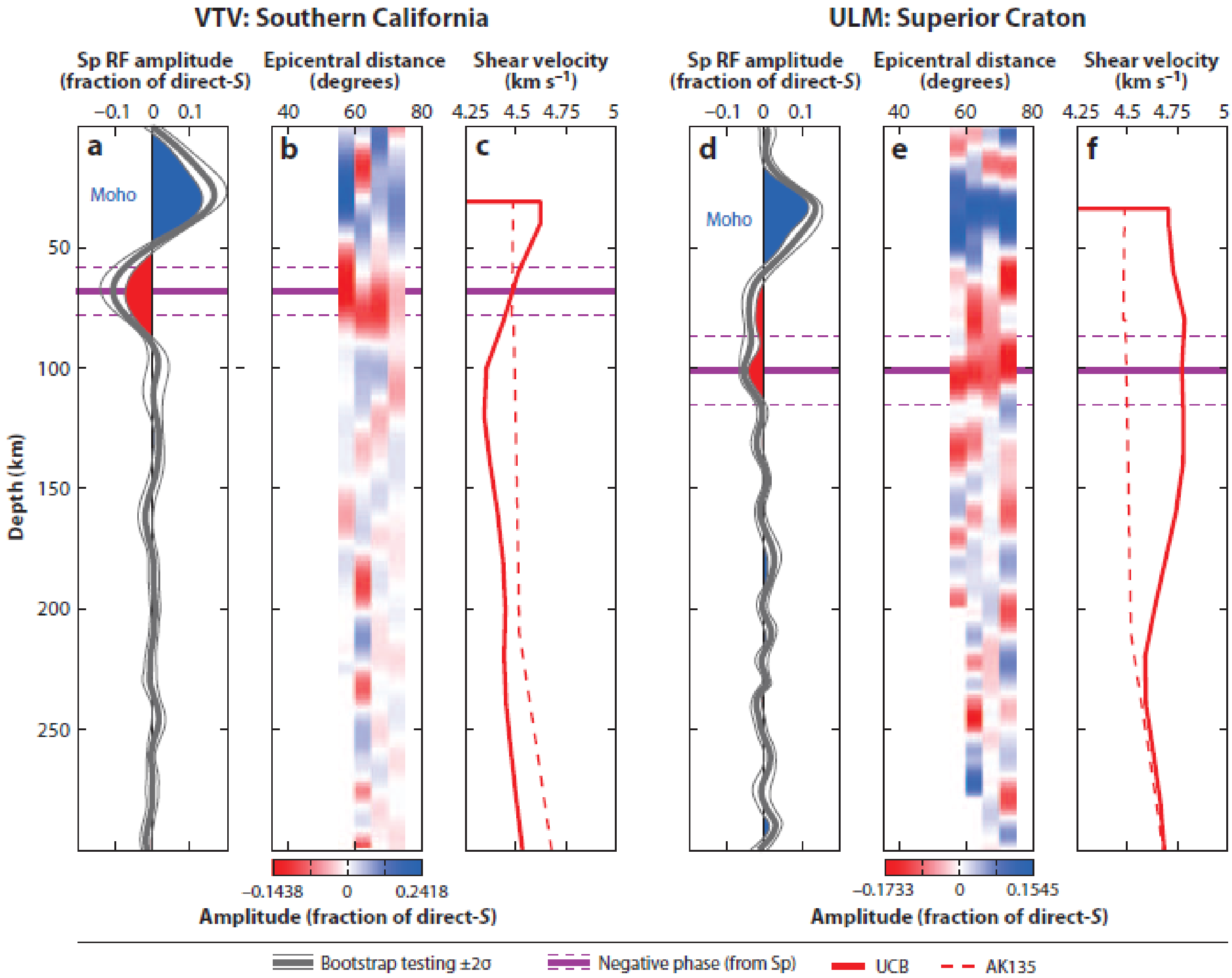

Fischer et al., 2010

LAB or MLD?

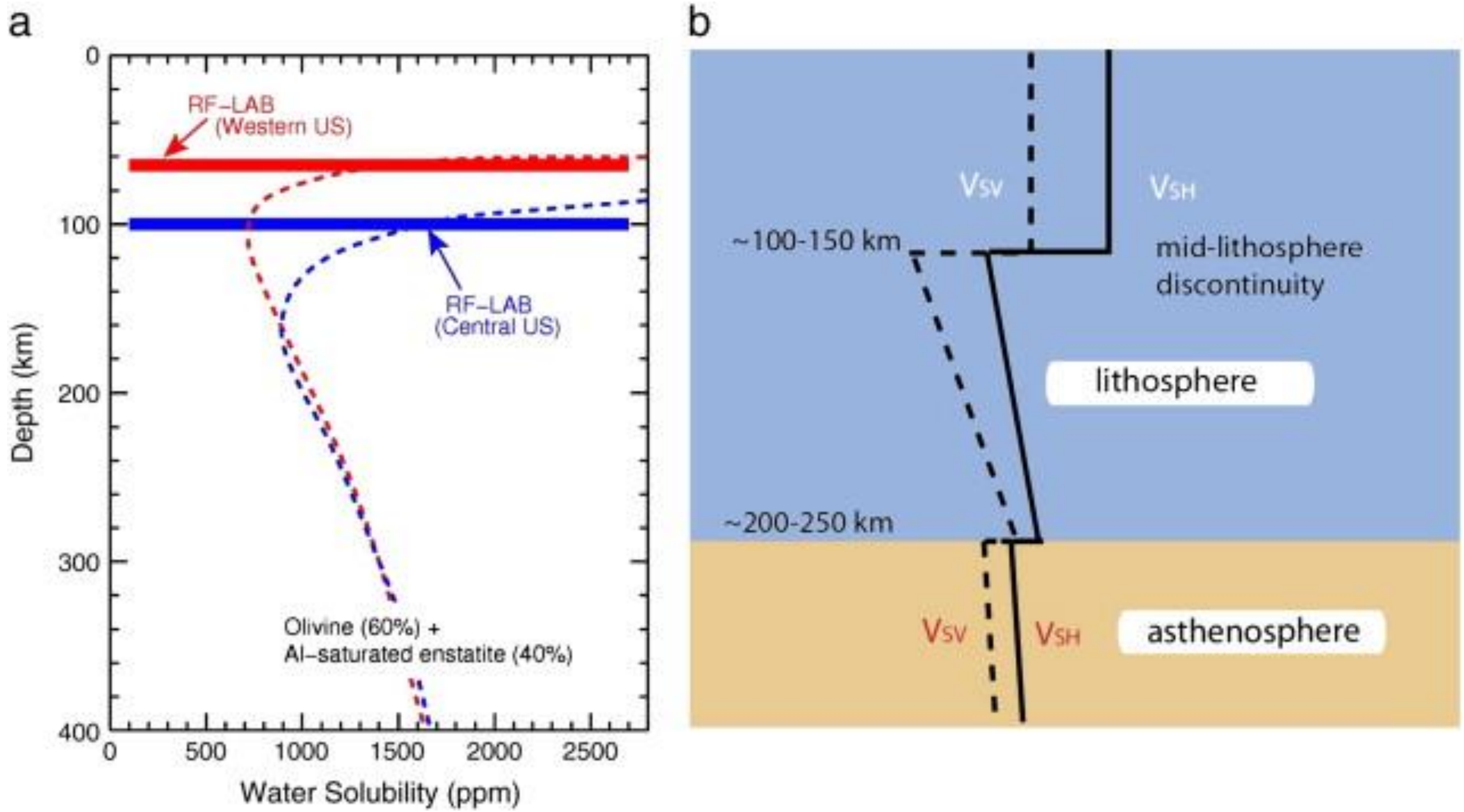

Kind et al.., 2012

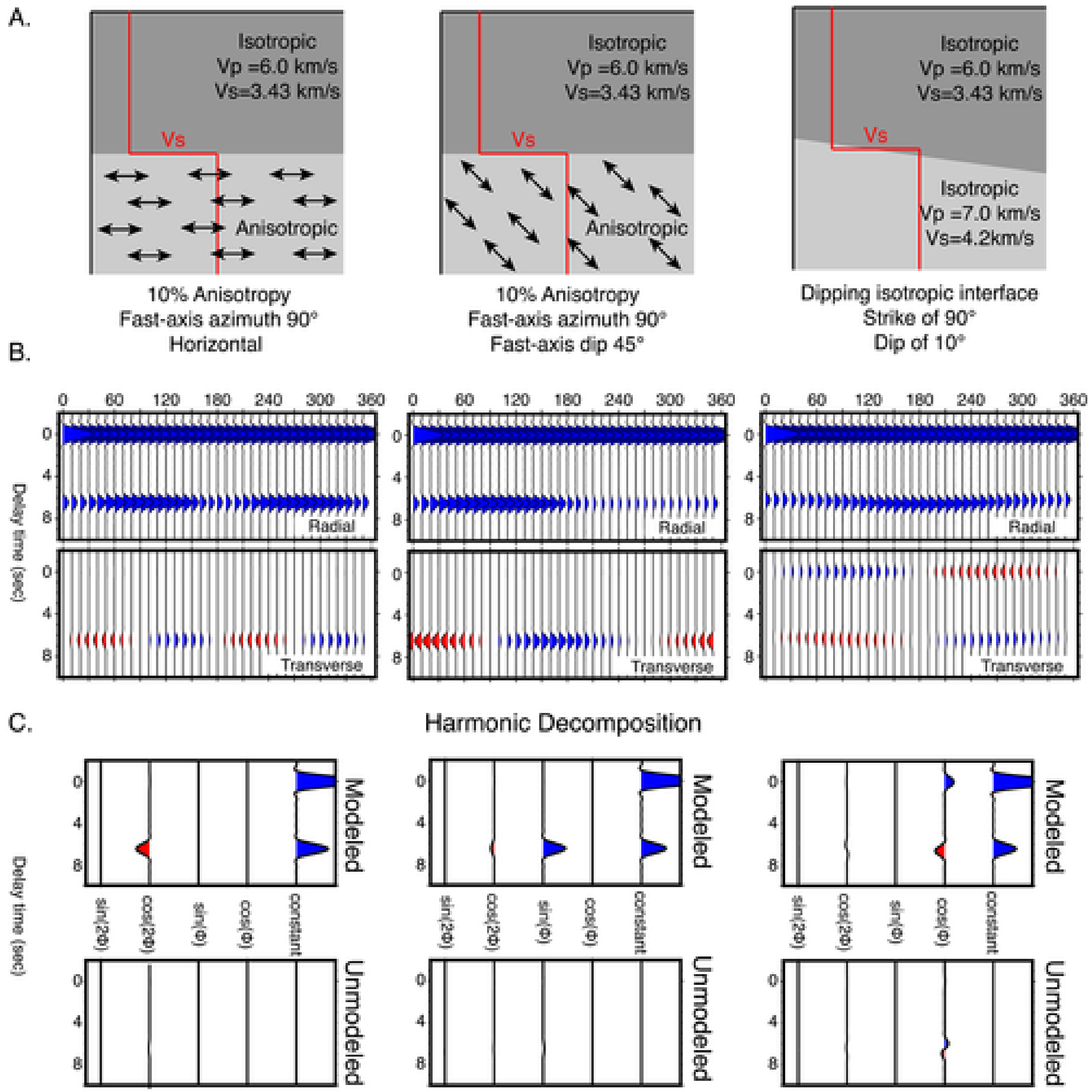

Ford et al.., 2016

Conclusion

RFs:

important constraints to characterize the LAB

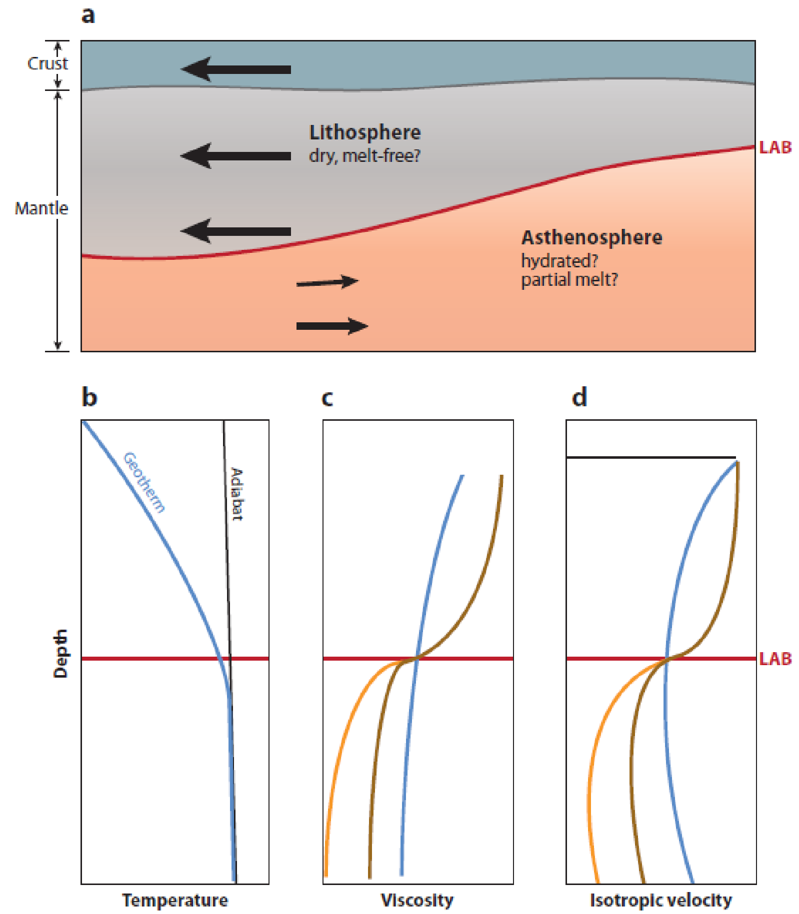

Figure 1

Schematic models of lithosphere-asthenosphere boundary (LAB) properties. (*a*) Depth profile through the lithosphere and asthenosphere. Arrows show the motion of a coherent lithospheric layer over a deforming asthenosphere. (*b*) Temperature as a function of depth. In the absence of other factors, the lithosphere would correspond to the cold thermal boundary layer represented by subadiabatic temperatures. (*c*) Mantle viscosity for three cases. Blue: the geotherm in panel *b*. Brown: the geotherm superimposed on a compositional difference at the LAB (dry lithosphere over hydrated asthenosphere). Orange: the latter case plus partial melt in the asthenosphere. (*d*) Isotropic shear velocity corresponding to the three cases in panel *c*. The black line schematically illustrates the velocity increase from the crust to the mantle.

UNIVERSITY OF OSLO

Figure 2.5-5: Transmitted and reflected waves for incident *P* and *SV* waves.

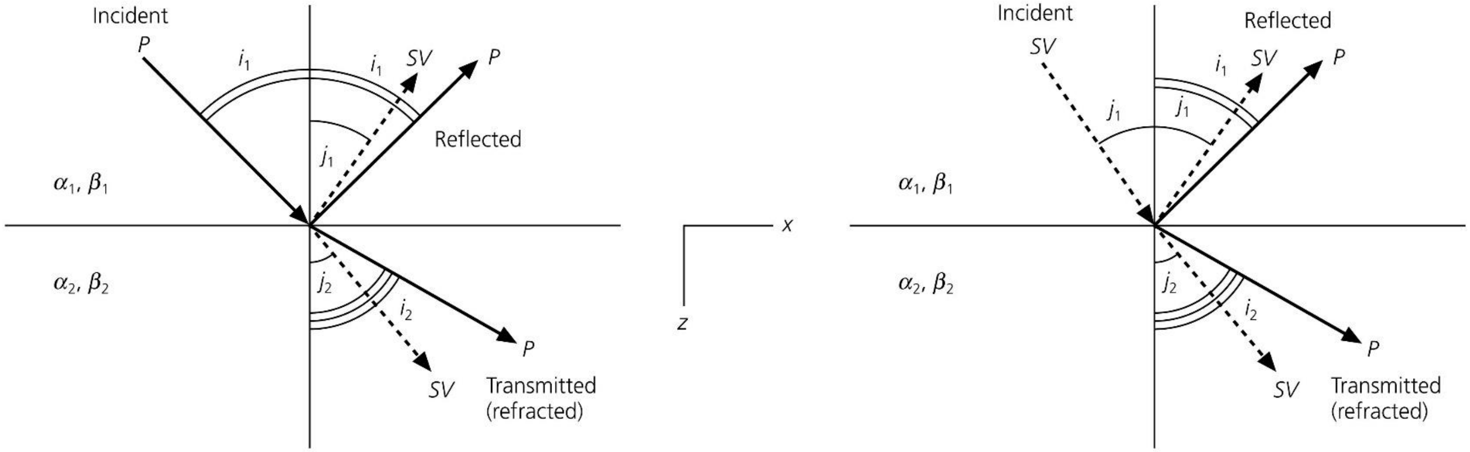

attempt at a standard moveout plot for narrow azimuthal range